

09.5

Fiber Optic SMS Sensor for Simultaneous Measurement of Strain and Curvature

© A.A. Markvart, L.B. Liokumovich, N.A. Ushakov

Peter the Great Saint-Petersburg Polytechnic University, St. Petersburg, Russia
E-mail: markvart_aa@spbstu.ru

Received July 21, 2021

Revised August 23, 2021

Accepted August 31, 2021

The article presents a fiber-optic sensor based on a singlemode–multimode–singlemode (SMS) structure for simultaneous measurement of strain and curvature. It is shown that the simultaneous demodulation of strain and curvature can be realized using the Fourier analysis of the recorded interference oscillations.

Keywords: optical fiber sensors, intermode interference, single mode–multimode–single mode, stretching, bending.

DOI: 10.21883/TPL.2022.15.55279.18969

Fiber optic sensors (FOSs) are the subject of active research due to their high potential accuracy, electromagnetic neutrality, compact size, multiplexing capability, and remote interrogation capability. FOSs allow to measure various physical influences, such as temperature, tension, bending, etc., which is necessary for various applications: from monitoring buildings and structures to medical diagnostics [1,2]. One of the most used types of FOS are sensors based on fiber interferometers or fiber Bragg gratings. However, typical disadvantages of such sensors are cross-sensitivity to various physical influences and the impossibility of their simultaneous measurements. To eliminate these disadvantages, it is necessary to use complex structures with various sensitive elements that have different sensitivities to the measured influences.

A promising type of FOS is the sensor based on the structure of singlemode–multimode–singlemode fiber [3,4]. The sensitive part here is a section of multimode fiber (MMF) with length of several centimeters to several tens of centimeters. This section is connected on both sides to single-mode fibers (SMF) for connection to the light source and the photodetector. The radiation of the first SMF excites several modes in the MMF, which, after passing through the entire length of the MMF, excite the fundamental mode of the second SMF. The field distribution at the MMF output is the result of mode interference and depends on the optical path difference (OPD) of the modes. When a physical influence is applied to the sensitive section, the OPD of the MMF mode changes, which leads to a change in the field at the MMF output and the power coming from the MMF to the second SMF, which is fixed by the photodetector. In fact, such a sensor is a variant of the intermode interferometer [5], so it can be called an intermode interferometer with a single mode connection (IISMC). Typically, such a sensor is interrogated by the method of spectral interferometry [6,7]: the dependence of the intensity level of the light transmitted through the IISMC on the wavelength $I(\lambda)$ is recorded.

It has been shown in a number of publications that it is possible to take into account the cross sensitivity of the sensor to several physical influences in the IISMC signal and measure them simultaneously [8–10]. In the work [8], the temperature-compensated IISMC bending sensor is demonstrated. In [9], simultaneous measurement of temperature and displacement caused by bending is implemented, and in [10] those of temperature and tension. However, at the moment, quite simple signal processing algorithms are used to demodulate the IISMC signal, such as tracking the shift of $I(\lambda)$ signal extrema and measuring their half-width. Due to the complex nature and behavior of the dependence $I(\lambda)$, such simple approaches are unlikely to become the basis for effective unified algorithms for determining perturbations. More detailed analysis of the IISMC signals, in particular the analysis of their spectra, can lead to better and more universal results. There are examples of applying sophisticated processing algorithms to the IISMC signal [11–13], but they have not yet been experimentally tested for simultaneous measurements of several physical effects. The present work is devoted to the experimental analysis of the IISMC signal using the Fourier transform (FT) to demonstrate the simultaneous measurement of tension and bending.

The possibility of separating the tension effect and bending is due to their different influence of the modes on the OPD. In the case of MMF stretching, the increments of the OPD modes are always practically proportional to the initial OPD modes with a coefficient independent of the mode numbers, and when MMF is bent, the situation depends on the type of fiber. For a parabolic fiber, there is also the proportionality factor that does not depend on the mode numbers, which prevents the implementation of multiparameter measurements [14]. In stepped MMFs, the proportionality factor depends on the mode numbers, which can be shown using numerical simulations. However, the present work is devoted to experimental demonstration of

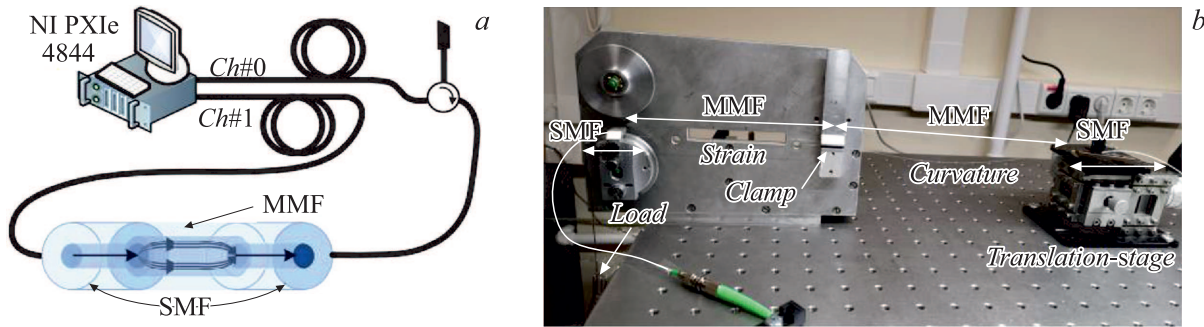


Figure 1. Interrogation scheme (a) of the intermode interferometer with single-mode connection (IISMIC) and a photograph of the experimental installation (b).

the possibility of simultaneous measurement of tension and bending using the analysis of $I(\lambda)$ spectra. At the same time, the theoretical consideration of this issue requires a separate study, since it is necessary to analyze not only the OPD modes, but a number of other factors that determine the complex structure of the signal $I(\lambda)$.

The diagram of the experimental installation is shown in Fig. 1. The fiber optic part of the IISMIC is implemented by welding the 32 cm length piece of Thorlabs FG050LGA multimode fiber with standard SMF-28 single-mode fibers. The fibers were welded with an automatic fusion splicer without any intentional displacements at the welding joint. In this case, only axisymmetric LP_{0p} modes of the multimode fiber are excited, which provides a smaller number of interference components in $I(\lambda)$ and makes the IISMIC signal more acceptable for processing. The IISMIC interrogation was carried out using the four-channel NI PXIe 4844 optical interrogator, which registers the spectral dependence of the reflection of the interrogated optical device in the region $1.51\text{--}1.59\ \mu\text{m}$ (scanning range $\Delta\lambda = 80\ \text{nm}$, step $d = 4\ \text{pm}$, number of points $N = 20\ 000$). Since this interrogator registers reflected optical radiation, the first channel of the interrogator was used as a light source to measure the spectral transmission of the IISMIC, and the zero channel was used to record the output signal of the IISMIC (Fig. 1, a). To eliminate the influence of reflection from the IISMIC with this connection the circulator and the absorbent fiber plug were used. As a result, the signal $I(\lambda)$ was recorded as a sequence of readings $I_i = I(\lambda_i)$, $i = 1, \dots, N$.

To implement the influences, the MMF was divided into two sections, one was subjected to tension, and the other to bending. This corresponds to the simultaneous action of bending and stretching on the IISMIC, since the change in the signal $I(\lambda)$ is formed by integral intermode phase delays and does not depend on the place of influence. At the same time, the division into sections made it possible to introduce independent and clearly controlled influences. The middle of the MMF was fixed with a clamp (Fig. 1, b). The SMF on the left side of the IISMIC was pressed against the roller, on which weights of different masses were attached, causing a certain stretching of the left section of the MMF. The SMF

on the right side of the IISMIC was fixed on the platform of the micro-positioner at a distance of $2A$ from the pressing point of the MMF middle. Since the length of the fibers in the right part of the IISMIC between the points was greater than $2A$, the fiber had a natural bend, which was controlled by shifting the micro-positioner platform. Wherein, one can approximately assume that the fiber is bent with a constant value of curvature ρ , the increment of which was estimated by the formula $2dA/(dA^2 + A^2)$ [8], where dA is offset of the micro-positioner platform.

Examples of initial signals $I(\lambda)$ for three sets of tension and bending curvature values are shown in Fig. 2, a. On the enlarged fragments, it is clearly seen that the shifts of dips and changes in their width caused by the influence have a different and difficult to predict character. Therefore, simple $I(\lambda)$ dependency processing methods to determine influences are unlikely to be efficient and universal. In this work, it is proposed to use the analysis of the $I(\lambda)$ dependence spectrum; for this, the FT was applied to the I_i sequence.

For interference of only two modes (two-beam interference) with OPD equal to L , the variable part of the signal $I(\lambda)$ is the oscillation $\cos(2\pi L/\lambda)$. If the change in wavelength $\delta\lambda = \lambda - \lambda_0$ is small in comparison with the center of the range λ_0 , then we obtain $\cos(2\pi L/\lambda) \approx \cos[(2\pi L/\lambda_0^2)\delta\lambda + \theta(L)]$, i.e. quasi-harmonic oscillation with frequency L/λ_0^2 and with initial phase $\theta(L)$. Therefore, applying the FT to the sequence I_i gives a sequence of readings S_i , where the index i can be associated with the values of the OPD. L , expressed as $L = i\lambda_0^2/\Delta\lambda$. It is also expediently to consider the amplitudes $S_{Ai} = |S_i|$ and the phases of the spectral components $\varphi_i = \arg[S_i]$.

Example of the experimental spectrum S_A is shown in Fig. 2, b. The horizontal axes indicate the numbers of readings i and the corresponding values L . The S_{Ai} maxima characterize the presence of interference of certain mode pairs in the I_i signal (components with close OPDs can merge due to the limited resolution of the OPD equal to $\Delta L = \lambda_0^2/\Delta\lambda \approx 30\ \mu\text{m}$). Note, that for the ranges of tensions and bendings of the MMF used in the experiments, the observed dependences S_{Ai} practically did not change.

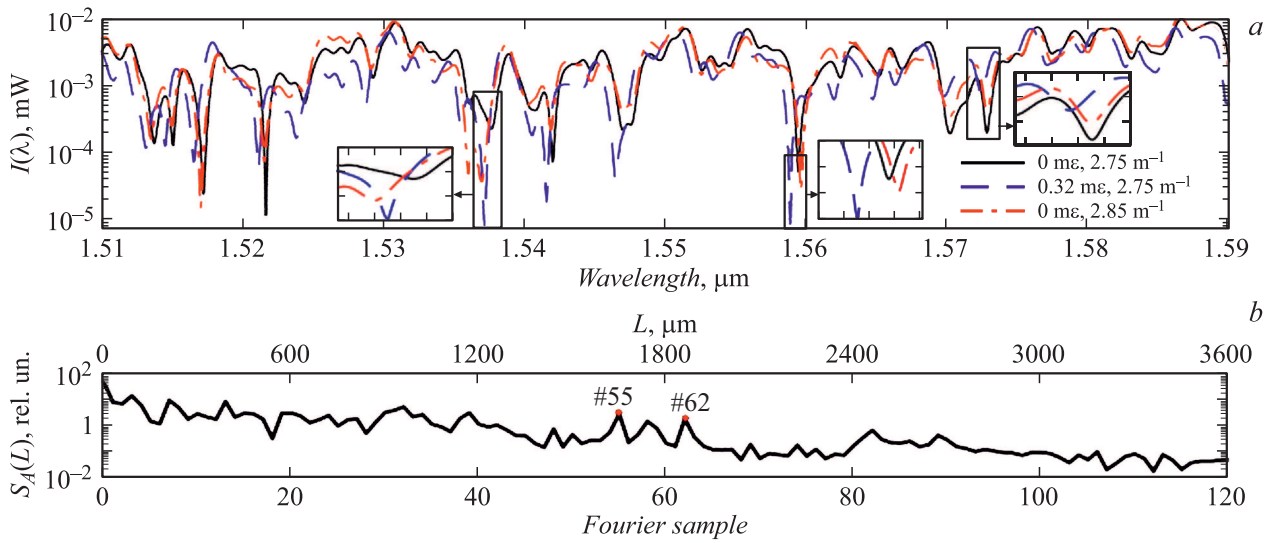


Figure 2. Experimental IISM signals (a) and their spectra (b).

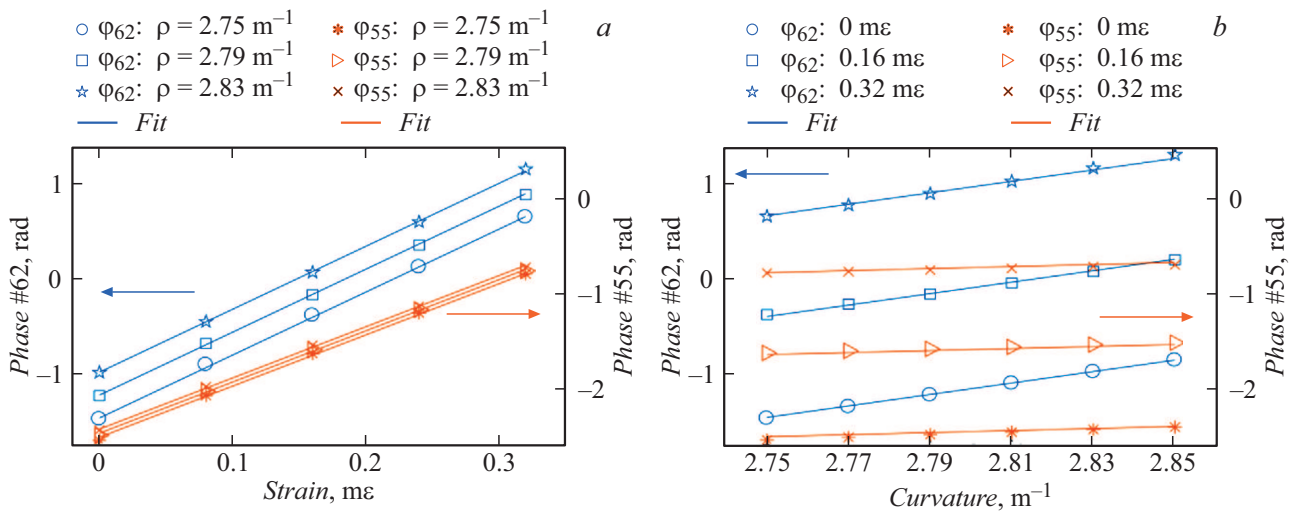


Figure 3. Dependences of φ_{55} and φ_{62} phases on tension (a) and on bending curvature (b).

In accordance with the proposed concept, to determine the influence of perturbations, two maxima S_{A1} and S_{A2} were chosen and the phases φ_1 and φ_2 were analyzed.

In the measurements carried out, the tension ε varied from 0 to $0.32 \text{ m}\varepsilon$ with the step of $0.08 \text{ m}\varepsilon$, and the bending curvature ρ varied from 2.75 to 2.85 m^{-1} with step 0.02 m^{-1} . As a result, 30 dependences I_i were recorded, which were then used to find the S_i spectra and the phases of the spectral components. As a result, based on the analysis of the dependence of the φ_i phases on the influences, two points of the spectrum (counts #55 and #62) were selected with the corresponding values of L_1 and L_2 equal to 1651 and $1861 \mu\text{m}$. At these points, characteristic maxima of the amplitude spectrum are observed (Fig. 2, b), and the dependences of the phases of these components on the influences showed better linearity.

Examples of the dependences of φ_{55} and φ_{62} on one of the parameters with a fixed value of the other are shown in Fig. 3, from which it is easy to see that the dependences are close to straight lines. Approximation of the dependences of φ_{55} and φ_{62} on various perturbations by the plane equation gives

$$\begin{aligned} \varphi_{55} &= -5.4692 + 5.4025\varepsilon + 1.0745\rho, \\ \varphi_{62} &= -18.0707 + 6.6437\varepsilon + 6.04\rho, \end{aligned} \quad (1)$$

where tension ε and bending curvature ρ are given in units of $[\text{m}\varepsilon]$ and $[\text{m}^{-1}]$, respectively. The corrected R^2 -parameter (determination coefficient) of the approximation of the two-dimensional dependence $\varphi(\varepsilon, \rho)$ by the plane was 0.9997 for φ_{55} and 0.9992 for φ_{62} , which demonstrates the high adequacy of approximation (1). Equations (1) are linearly independent: the condition number for (1) is 4, which indicates the low sensitivity of the solution to small errors in

the phases of the Fourier readings. To estimate tension and bending from the signals of this IISMC scheme, the system of equations (1) can be solved in the following form:

$$\begin{aligned}\varepsilon &= 0.534 + 0.237\varphi_{55} + 0.0421\varphi_{62}, \\ \rho &= 2.4 + 0.261\varphi_{55} + 0.212\varphi_{62}.\end{aligned}\quad (2)$$

Thus, using the example of MMF tension and bending in the IISMC scheme, the possibility of simultaneously measuring several physical parameters using the IISMC interrogation with wavelength scanning, calculating the spectrum of the obtained oscillations $I(\lambda)$, and analyzing the phases of the pair of spectral components, are experimentally demonstrated. Such processing of the IISMC signal, which is complex in appearance and behavior, makes it possible to extract from it information directly related to the change in the OPD of the MMF. modes. In this case, the operations used are relatively simple standard transformations of the initially recorded signal $I(\lambda)$. Therefore, the proposed approach to the implementation of measurements with IISMC can become the basis for an effective unified principle for the implementation of measurements in structures based on intermode interferometers with the single-mode connection, including simultaneous measurements of different physical quantities.

Funding

The study was funded by RFBR within the framework of the scientific project № 19-32-90262.

Conflict of interest

The authors declare that they have no conflict of interest.

References

- [1] I.R. Matias, S. Ikezawa, J. Corres, *Fiber optic sensors. Current status and future possibilities* (Springer International Publ., Switzerland, 2017). DOI: 10.1007/978-3-319-42625-9
- [2] N.A. Ushakov, A.A. Markvart, D.D. Kulik, L.B. Liokumovich, *Photonics*, **8** (5), 142 (2021). DOI: 10.3390/photonics8050142
- [3] A. Kumar, R.K. Varshney, S. Antony, P. Sharma, *Opt. Commun.*, **219** (1-6), 215 (2003). DOI: 10.1016/S0030-4018(03)01289-6
- [4] Q. Wu, Y. Qu, J. Liu, J. Yuan, S.P. Wan, T. Wu, X.D. He, B. Liu, D. Liu, Y. Ma, Y. Semenova, P. Wang, X. Xin, G. Farrell, *IEEE Sens. J.*, **21** (11), 12734 (2020). DOI: 10.1109/JSEN.2020.3039912
- [5] O.I. Kotov, M.A. Bisyarin, I.E. Chapalo, A.V. Petrov, *J. Opt. Soc. Am. B*, **35** (8), 1990 (2018). DOI: 10.1364/JOSAB.35.001990
- [6] S.M. Tripathi, A. Kumar, R.K. Varshney, Y.B.P. Kumar, E. Marin, J.P. Meunier, *J. Light. Technol.*, **27** (13), 2348 (2009). DOI: 10.1109/JLT.2008.2008
- [7] M. Kumar, A. Kumar, S.M. Tripathi, *Opt. Commun.*, **312**, 222 (2014). DOI: 10.1016/j.optcom.2013.09.034
- [8] S. Silva, O. Frazão, J. Viegas, L.A. Ferreira, F.M. Araújo, F.X. Malcata, J.L. Santos, *Meas. Sci. Technol.*, **22** (8), 085201 (2011). DOI: 10.1088/0957-0233/22/8/085201
- [9] Q. Wu, A.M. Hatta, P. Wang, Y. Semenova, G. Farrell, *IEEE Photon. Technol. Lett.*, **23** (2), 130 (2011). DOI: 10.1109/LPT.2010.2093515
- [10] C. Lu, J. Su, X. Dong, T. Sun, K.T.V. Grattan, *J. Light. Technol.*, **36** (13), 2796 (2018). DOI: 10.1109/JLT.2018.2825294
- [11] Y. Cardona-Maya, I. Del Villar, A.B. Socorro, J.M. Corres, I.R. Matias, J.F. Botero-Cadavid, *J. Light. Technol.*, **35** (17), 3743 (2017). DOI: 10.1109/JLT.2017.2719923
- [12] A. Ahrens, A. Sandmann, K. Bremer, B. Roth, S. Lochmann, *Proc. SPIE*, **9634**, 96345W (2015). DOI: 10.1117/12.2195114
- [13] A.V. Petrov, I.E. Chapalo, M.A. Bisyarin, O.I. Kotov, *Appl. Opt.*, **59** (33), 10422 (2020). DOI: 10.1364/AO.400345
- [14] A.A. Markvart, L.B. Liokumovich, N.A. Ushakov, *Nauch.-tekhn. vedomosti SPbGPU Fiz.-mat. nauki*, **14** (2), 104 (2021) (in Russian). DOI: 10.18721/JPM.14209